DYNAMICS OF GROWING CELL POPULATIONS

N. BESSONOV, P. KURBATOVA, V. VOLPERT

1. Introduction

In this paper we develop hybrid discrete-continuous models in order to investigate dynamics of cell populations in biological tissues. In hybrid methods cells are considered as discrete objects described either by cellular automata or by various lattice or off-lattice models while intra-cellular and extra-cellular concentrations are described with continuous models, ordinary or partial differential equations. Such approaches receive more and more attention in modelling cellular systems [3]. Cellular automata are applied to model tumour invasion in [8] where tumour is considered as a collection of many individual cancer cells that interact and modify the environment through which they grow and migrate. The authors examine how individual-based cell interactions can affect the tumour morphology. In the article [2] hybrid models are applied to investigate the influence of the microenvironement on tumour invasion, cell-cell communication and competition leading to the initiation and growth of epithelial tumours, and to evolution of cell phenotypes/genotypes arising in tumours growing in different oxygen concentrations. Cellular automata are also used in modelling of adhesion and chemotaxis [9]

In lattice-free models, cells are considered as discrete objects which move according to the forces acting on them from the surrounding medium. Modelling of cells growing in tissue on a flat substrate is presented in the work by D. Drasdo [5]. J. C. Dallon [7] models distyostelium discoideum where individual amoebae are treated as discrete entities. They move and communicate with each other through a diffusible chemical. The second model describes scar tissue formation.

In this work we introduce and study the hybrid model with off-lattice cell dynamics. Cells can interact with each other and with the surrounding medium mechanically and biochemically, they can divide, differentiate and die due to apoptosis. Cell behavior is determined by intra-cellular regulatory networks described by ordinary differential equations and by extra-cellular bio-chemical substances described by partial differential equations. Each cell has ability of growing, moving, dividing and exchanging biochemical substances with surrounding medium.

We describe motion of each cell by the displacement of its center. By Newton's second law

$$m\ddot{x}_i + \mu m\dot{x} - \sum_{j\neq i} f(d_{ij}) = 0, \tag{1.1}$$

where m is the mass of the particle, the second term in the left-hand side describes the friction by the surrounding medium. Dissipative forces can also be written in a different form.

Intra-cellular regulatory networks for the i-th cell are described by a system of ordinary differential equations

$$\frac{du_i}{dt} = F(u_i, u), \tag{1.2}$$

where u_i is a vector of intra-cellular concentrations, u is a vector of extra-cellular concentrations, F is the vector of reaction rates which should be specified for each particular application. The concentrations of the species in the extra-cellular matrix is described by the diffusion equation

$$\frac{\partial u}{\partial t} = D\ \Delta u + G(u, c), \tag{1.3}$$

where c is the local cell density, G is the rate of consumption or production of these substances by cells. These species can be either nutrients coming from outside and consumed by cells or some other bio-chemical products consumed or produced by cells. In particular, these can be hormones or other signaling molecules that can influence intra-cellular regulatory networks. In some cases, convective motion of the medium should be taken into account.

The paper is organized as follows. In Section 2 we discuss a hybrid model for multi-scale modelling of cells population. In Section 3 we start with the 1D case and study with three model problems. In the first one, each cell can self-renew or die by apoptosis. In the second model, we study the model where cells self-renew or differentiate into another type of cells. Finally, in the last model, we investigate the case where cells can divide or be in a quiescent state. In Section 4 we extend our results to the two dimensional case and we introduce a model of tumor growth.

2. Dissipative particle dynamics and continuous models

2.1. **From cells to particle dynamics.** Consider two elastic balls with the centers at the points x_1 and x_2 and with the radii, respectively, r_1 and r_2. If the distance d_{12} between the centers is less than the sum of the radii, $r_1 + r_2$, then there is a repulsive force between them f_{12} which depends on the distance d_{12}.

If a particle with the center at x_i is surrounded by several other particles with the centers at the points x_j, $j = 1, ..., k$, then we consider the pairwise forces f_{ij} assuming that they are independent of each other. This assumption corresponds

to small deformation of the particles. Hence, we find the total force F_i acting on the i-th particle from all other particles,

$$F_i = \sum_{j \neq i} f_{ij}.$$

The motion of the particles can now be described as the motion of their centers.

2.2. **From discrete to continuous model.** Consider a system of N particles in the plane. Denote their coordinates by $x_1, ..., x_n$. Here x_i is a two-component vector. Suppose that all particles have the same mass m and consider the equation of motion of the i-th particles in the form

$$\ddot{x_i} + \mu m \dot{x_i} + \sum_{j \neq i} f_{ij} = 0. \tag{2.4}$$

The dot denotes the derivative with respect to time, $\ddot{x_i}$ is the particle acceleration, $\dot{x_i}$ is its speed. The second term in the left-hand side of this equation describes dissipation due to friction, the last term is the sum of forces acting on this particle from all other particles.

The force f_{ij} acting between the particles i and j can be expressed through the potential: $f_{ij} = -m\nabla\phi(|x - x_j|)_{x=x_i}$. Then

$$\ddot{x_i} + \mu \dot{x_i} + \nabla \left(\sum_{j \neq i} \phi(|x - x_j|) \right)_{x=x_i} = 0, \quad 1, ..., N. \tag{2.5}$$

Consider a square grid with the mesh points $\bar{x}_i$ and the step δx. Denote by s_i the square with the side 2 δx and the center at the point $\bar{x}_i$. Let $x_{i1}, ..., x_{ik} \in s_i$. Let us introduce velocity and density at the grid points:

$$v_i = \frac{1}{k} \sum_{j=1}^{k} \dot{x}_{ij}, \quad \rho_i = \frac{k}{|s_i|},$$

where $|s_i| = 4(\delta x)^2$ is the area of s_i. Then

$$\sum_j \phi(|x - x_j|) \approx \sum_m \phi(|x - \bar{x}_m|)\rho_m |s_m| \approx U(x),$$

where

$$U(x) = \int \phi(|x - x'|)\rho(x')dx'.$$

Taking a sum of equations (2.5) with respect to the points inside s_i, we obtain the discrete equation

$$\rho_i \frac{dv_i}{dt} + \mu \rho_i v_i + \rho_i (\nabla U)_i = 0, \tag{2.6}$$

where we use the approximation $\frac{1}{k} \sum_{j=1}^{k} \phi(|x_j - \bar{x}_m|) \approx \phi(|\bar{x}_i - \bar{x}_m|)$. Averaged equation (2.6) may not be equivalent to (2.5). Two particles $x_j, x_k \in s_i$ with

opposite velocities cancel in (2.6) but not in (2.5). They result in the momentum transfer and can be taken into account in (2.6) by additional dissipative terms. In numerical simulations, the equivalence of these equations can be provided if we take an average velocity with respect to some ensembles of particles.

Consider the continuous analogue of discrete equation (2.6)

$$\rho\frac{dv}{dt} + \mu\rho v + \rho(\nabla U) = 0. \tag{2.7}$$

This equation of motion should be completed by the equation of mass conservation:

$$\frac{\partial\rho}{\partial t} + \nabla.(\rho v) = 0. \tag{2.8}$$

We can write equation (2.7) in the form

$$\rho\Big(\frac{\partial v}{\partial t} + v.\nabla v\Big) + \mu\rho v + \nabla p - U\nabla\rho = 0, \tag{2.9}$$

where p is the pressure, $p = \rho U$. This equation is nonlocal because the potential U contain the integral. Using the Taylor expansion of the density $\rho(x')$ around the point x and keeping the terms up to the second order, we obtain

$$\rho\Big(\frac{\partial v}{\partial t} + v.\nabla v\Big) + \mu\rho v + \nabla p - K\Delta\rho\nabla\rho = 0. \tag{2.10}$$

The pressure in this equation is different in comparison with the previous one but we keep for it the same notation. This equation does not contain the potential anymore. Therefore, we cannot express the pressure through it, and we need to complete system (2.8), (2.10) by an equation of state, $p = p(\rho)$. In the case $\mu = 0$ and $K = 0$, (2.10) is the Euleur equation and system (2.8), (2.10) becomes the classical model of gas dynamics.

2.3. **1D test case.** We will study in this section the test case where a 1D interval is filled by cells of two types, A and B. Cells of the type A divide and after each division produce one cell A and one cell B. The cells of the type B do not divide. If initially there is a unique cell of the type A, then it will remain unique and the interval will be filled by cells of the type B. In the continuous analogue of this model, the cell A is a point source. We will compare the numerical solution of the cell problem with an analytical solution of the continuous problem.

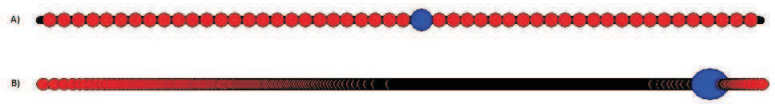

FIGURE 1. Example of particle dynamics simulation. Dividing cell (type A) is blue, not dividing cells (type B) are red.

In the 1D case, the last term in the left-hand side of the equation (2.10) has the form $K\rho'\rho''$ and can be included in the pressure. Consider the equation

$$\rho\frac{dv}{dt} + \mu\rho v + p' = 0. \tag{2.11}$$

This equation of motion should be completed by the equation of mass conservation:

$$\frac{d\rho}{dt} + \frac{\partial(\rho v)}{\partial x} = J, \tag{2.12}$$

where J the source of new particles (dividing cell). Let us consider the stationary case. Then we obtain

$$\mu(\rho v)' + p'' = 0, \tag{2.13}$$

$$p'' = -\mu J. \tag{2.14}$$

Cell division results in the mechanical interactions and the consequence their motion. This motion changes the position of the dividing cells. Thus, we come to the problem about the motion of point sources. Consider a 1D example where an analytical solution can be easily found:

$$p'' = -a\delta(x - \xi(t)), 0 < x < L, p(0) = p(L) = 0 \tag{2.15}$$

where $\xi(t)$ is a position of the point source. Let us introduce the function

$$p_0(x) = \begin{cases} \frac{a}{2}(x - \xi) + 1, x < \xi \\ \\ \frac{a}{2}(\xi - x) + 1, x > \xi \end{cases} \tag{2.16}$$

and put $p = p_0 + p_1$. Then $p_1'' = 0$ and

$$\begin{cases} p_1(0) = -p_0(0) = -1 + \frac{a\xi}{2}, \\ p_1(L) = -p_0(L) = -1 + \frac{a}{2}(L - \xi). \end{cases}$$

We find

$$p_1(x) = \frac{\frac{a}{2}(L - \xi) - \frac{a\xi}{2}}{L}x + (\frac{a\xi}{2} - 1).$$

From (2.11) we obtain,

$$\xi'(t) = -\frac{p'(\xi(t))}{\mu\rho}.$$

Consider when $\rho = 1$. The analytical solution of this equation is

$$\xi(t) = (\xi(t_0) - \frac{L}{2})e^{\frac{a}{\mu L}(t - t_0)} + \frac{L}{2}.$$

We carry out the 1D simulation where cells can move along the interval of a fixed length L. We note that only two nearest particles can interact. We consider

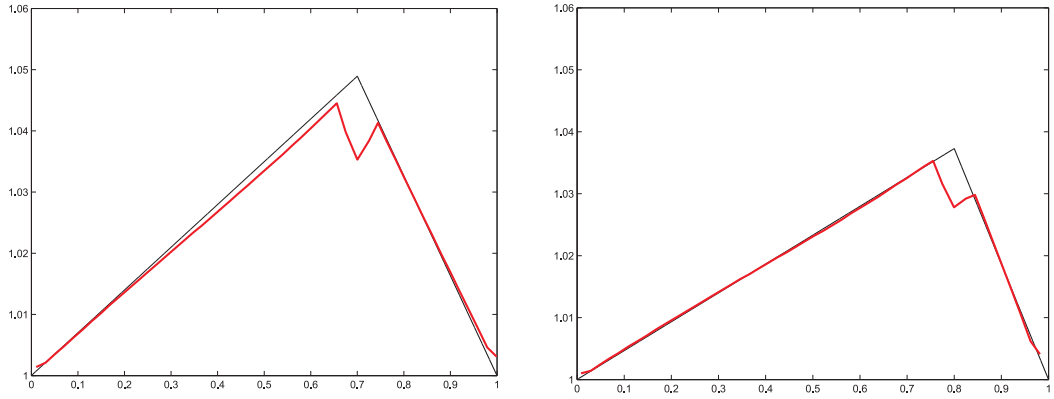

(a) (b)

FIGURE 2. Pressure distribution at two consecutive moments of time found analytically (black line) and numerically (red line); μ= 10 000, K= 200, h_0=0.01, h_1= 0.005, a=0.233.

the equation of motion (2.4). The force between two particles is considered in the form

$$f_{ij} = \begin{cases} K\frac{h_0-h_{ij}}{h_{ij}-(h_0-h_1)}, \ h_0-h_1 < h_{ij} < h_0, \ j = i \pm 1 \\ 0, \ h_{ij} \geq h_0 \end{cases} \tag{2.17}$$

Here h_{ij} is the distance between the particles i and j, h_0 is a diameter, $h_0 - 2h_1$ is incompressible part of each particle. This means that the distance between the centers of the particles can not be less than $h_0 - 2h_1$.

We put the dividing particle in the middle of the interval (Figure 1A). In the beginning we keep it fixed. It divides and fills the whole interval by the particles of the type B which do not divide. Then we detach the dividing particle. It starts moving to the boundary due to the pressure gradient (Figure 1B). Figure 2 shows the pressure distribution found numerically in particle dynamics and analytically. When the value of coefficient K is sufficient large (Figure 2), that is the medium is weakly compressible, then the numerical and analytical results are in a good agreement. If the value of coefficient K is smaller then the difference between numerical and analytical results is more more essential (Figure 3).

In spite of the good agreement for the pressure distribution, there is a big difference in the speed of the dividing cell found analytically and numerically (Figure 4). A possible explanation can be related to the fact that the analytical solution is found under the quasi-stationary approximation. It may not be well applicable for particle dynamics because of the periodic oscillations caused by cell division.

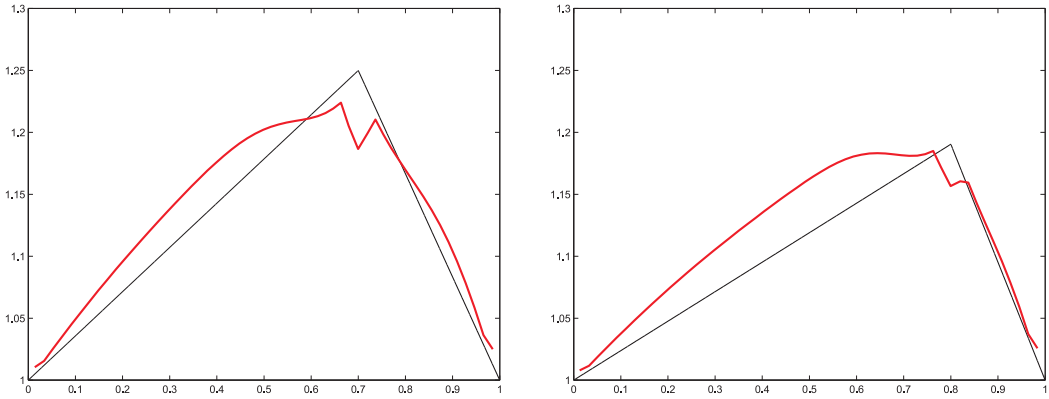

(a) (b)

FIGURE 3. Pressure distribution at two consecutive moments of time found analytically (black line) and numerically (red line); μ= 20 000, K= 50, h_0=0.01, h_1= 0.005, a=1.19.

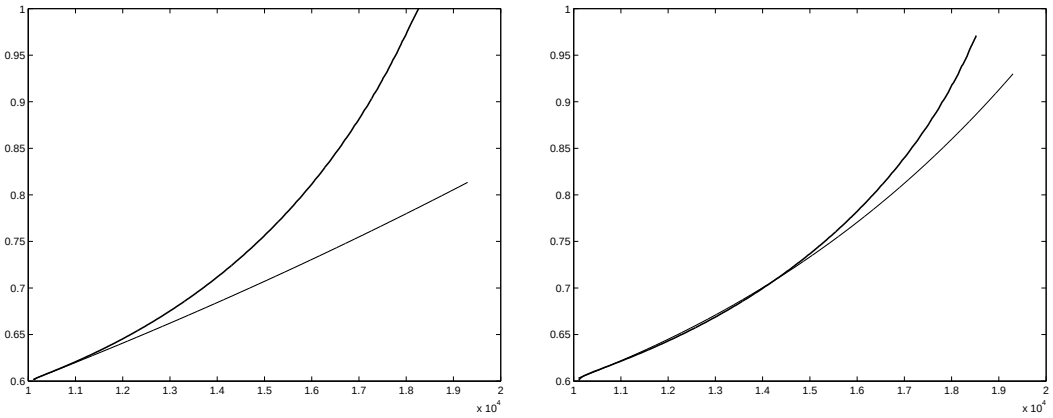

(a) K=300, a=0.304, $\xi'(t_0)$=2·10^{-5}, $\xi(t_0)$=0.604 (b) K=50, a=1.19, $\xi'(t_0)$=2·10^{-5}, $\xi(t_0)$=0.607

FIGURE 4. Coordinate of the growing particle as a function of time; numerical simulations (upper curve), the analytical solution (lower curve), μ= 20 000, h_0=0.01, h_1= 0.005.

3. 1D HYBRID MODELS

3.1. **Cell differentiation and apoptosis.** In this section we consider the complete model (1.1)-(1.3). We begin with the 1D model example where cells can move along the real line. Each cell can divide and die by apoptosis. After division cell gives two cells identical to itself. We suppose that cell division and death

are determined by some bio-chemical substances produced by the cells themselves. We consider the case where there are two such substances, u and v, which influence cell division and death. We come to the following system of equations:

$$\begin{cases} \dfrac{du}{dt} = d_1 \frac{\partial^2 u}{\partial x^2} + b_1 c - q_1 u, \\ \\ \dfrac{dv}{dt} = d_2 \frac{\partial^2 v}{\partial x^2} + b_2 c - q_2 v. \end{cases} \tag{3.18}$$

These equations describe the evolution of the extracellular concentrations u and v with their diffusion, production terms proportional to the concentration of cells c and with the degradation term. The equations above are completed by the no-flux boundary conditions.

Intra-cellular concentrations u_i and v_i in the i-th cell are described by the equations:

$$\begin{cases} \dfrac{du_i}{dt} = k_1^{(1)} u(x,t) - k_2^{(1)} u_i(t) + H_1, \\ \\ \dfrac{dv_i}{dt} = k_1^{(2)} v(x,t) - k_2^{(2)} v_i(t) + H_2. \end{cases} \tag{3.19}$$

The first term in the right-hand side of the first equation shows that the intracellular concentration u_i grows proportionally to the value of the extra-cellular concentration $u(x,t)$ at the space point x_i where the cell is located. These equations contain the degradation terms and constant production terms, H_1 and H_2. When a new cell appears, we put the concentrations u_i and v_i equal zero.

If the concentration u_i attains some critical value u_c, then the cell divides. If v_i becomes equal v_c, the cell dies. Consider first the case where $k_1^{(1)} = k_1^{(2)} = k_2^{(1)} = k_2^{(1)} = 0$. Then u_i and v_i are linear functions of time which reach their critical values at some moments of times $t = \tau_u$ and $t = \tau_v$, respectively. If $\tau_u < \tau_v$, then all cells will divide with a given frequency, if the inequality is opposite, then all cells will die. We notice that if $k_1^{(2)}$ equals zero, then the extracellular concentration v does not influence the evolution of v_i.

Next, consider the case where $k_1^{(1)}$ is different from zero. If it is positive, then cells stimulate proliferation of the surrounding cells, if it is negative, they suppress it. Both cases can be observed experimentally. We restrict ourselves here by the example of negative $k_1^{(1)}$. All other coefficients remain zero. Therefore, cells have a fixed life time. If they do not divide during this time, they die.

We carry out the 1D simulation where cells can move along the real line. Initially, there are two cells in the middle of the interval. Figure 5 shows the evolution of this population in time. Each blue dot shows one cell. For each moment of time (vertical axis) we observe the distribution of cell population in space (horizontal axis).

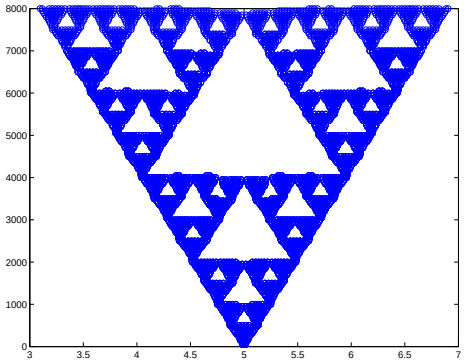

(a) $k_1^{(1)} = -5 \cdot 10^{-3}$, $V_{cr} = 2$, $D_1 = 0.0001$, $b_1 = 0.2$

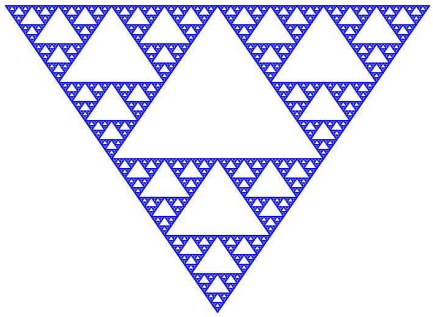

(b) Serpinsky carpet - fractal set

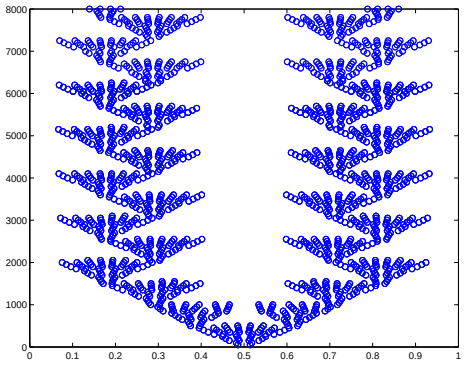

(c) $k_1^{(1)} = -5.5 \cdot 10^{-3}$, $V_{cr} = 2$, $D_1 = 0.0001$, $b_1 = 0.2$

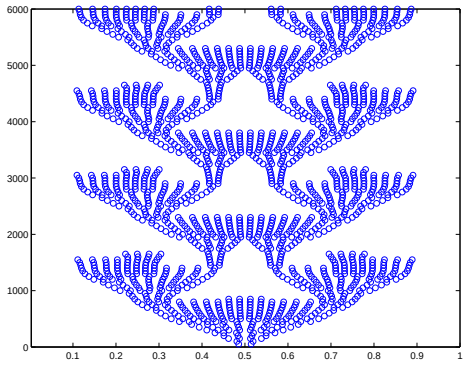

(d) $V_{cr} = 4$, $k_1^{(1)} = -5 \cdot 10^{-3}$, $D_1 = 10^{-3}$,$b_1 = 3.1$

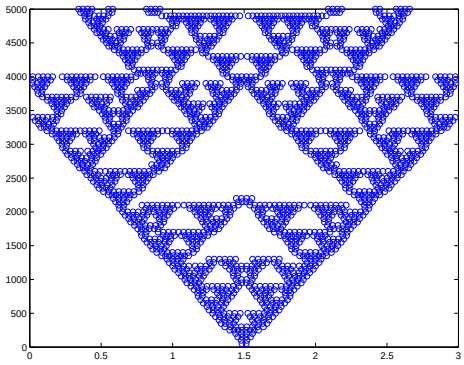

(e) $V_{cr} = 1.01$, $k_1^{(1)} = 10^{-4}$, $D_1 = 0.0001$, $b_1 = 0.2$

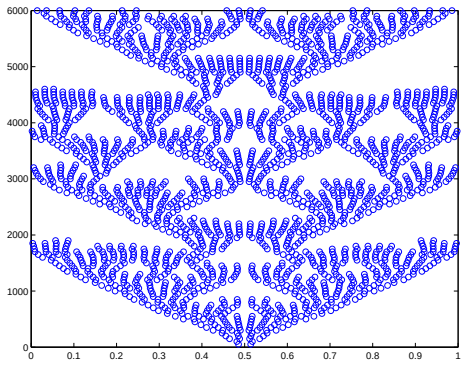

(f) $V_{cr} = 3$, $k_1^{(1)} = -5 \cdot 10^{-3}$, $D_1 = 0.0001$, $b_1 = 0.2$

FIGURE 5. Evolution of cell population where $k_2^{(1)} = k_1^{(2)} = k_2^{(2)} = 0$, $K_3 = 10^{-3}$, $H_1 = 0.1$, $H_2 = 0.01$, $b_2 = 0.1$, $q_1 = 0.02$, $q_2 = 0.0001$, $D_2 = 1$.

The distribution of u in the extracellular matrix is shown in Figure 6. It corresponds to the simulation shown in Figure 5 (e). This cell population spreads in space. The evolution of u in time corresponds to this propagation.

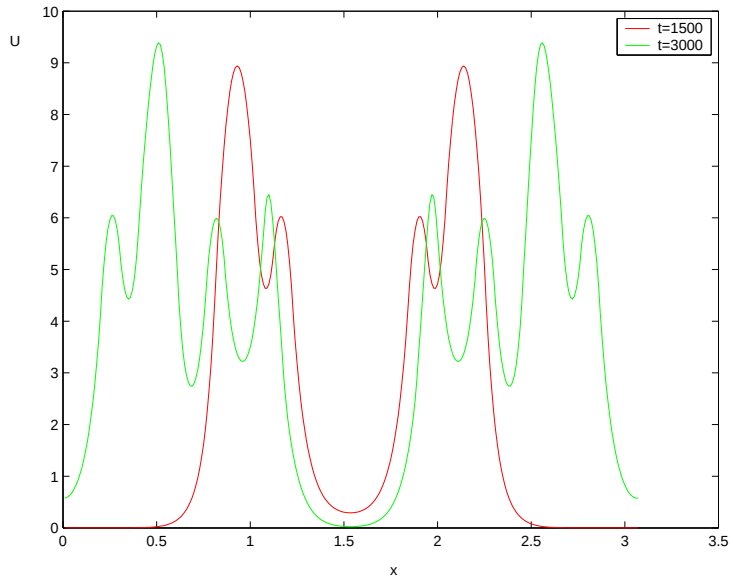

FIGURE 6. Distribution of u at different moments of time for the values of parameters $k_2^{(1)} = k_1^{(2)} = k_2^{(2)} = 0$, $K_3 = 10^{-3}$, $H_1 = 0.1$, $H_2 = 0.01$, $b_2 = 0.1$, $q_1 = 0.02$, $q_2 = 0.0001$, $D_2 = 1$, $V_{cr} = 1.01$, $k_1^{(1)} = 10^{-4}$, $D_1 = 0.0001$, $b_1 = 0.2$.

Dynamics of the cell population in Figure 5 (a) can be characterized by two main properties. First of all, it expands to the left and to the right with approximately constant speed. Second, the total population consists of relatively small sub-populations. Each of them starts from a small number of cells. Usually, these are two most right and left cells from the previous sub-population. During some time, the sub-population grows, reaches certain size and disappears giving birth to new sub-populations.

This behavior can be explained as follows. The characteristic time of cell division is less than of cell death. When the cell sub-population is small, the quantity of u is also small, and its influence on cell division is not significant. When the sub-population becomes larger, it slows down cell division because of growth of u. As a result the sub-population disappears. The outer cells can survive because the level of u there is less.

The geometrical pattern of cell distribution for these values of parameters reminds Serpinsky carpet (Figure 5, b), an example of fractal sets. It is obtained from an equilateral triangle by consecutive removing some of its parts. At the first step, the central triangle is removed. At the second step, the central part of each remaining triangle is removed and so on. In the case of cellular pattern, the

minimal triangle is determined by the cell size. Since this patterns grows with time, we can scale it to a triangle of a constant size. In this case, we obtain a decreasing sequence of removed (white) triangles, as it is the case for Serpinsky carpet.

The pattern of cell distribution depends on the parameters. Other examples are shown in Figure 5. The cell population in Figure 5 (c,d) remains bounded, and the pattern is time periodic. In the simulation shown in Figure 5 (a,e,f) the cell population grows with approximately constant speed.

3.2. **Cell division and differentiation.** In this model we describe extra-cellular and intra-cellular concentrations by equations (3.18) and (3.19). When v_i becomes equal to v_c, cells differentiate into another type of cells. The new type of cells do not have the ability to grow and divide. Figure 7 presents the evolution of the cell population depending on the critical value of v_c. We begin the simulation with two cells in the middle of the interval. The cell population starts growing. When it is small, the quantity of u produced by cells is also small, and its influence on cell division is not significant. When the population becomes larger, there is more u in the extracellular matrix. It slows down cell division. As a result, the concentration v_i attains the critical value v_c faster than u_i reaches u_c. Then the cells start to differentiate. When the critical value v_c is small (Figure 7, a) all cells finally differentiate into another cell type. If we increase the critical value v_c (Figure 7, b), then there is a stationary group of differentiated cells in the middle of interval. Other differentiated cells periodically appear from the right and from the left, they move towards the borders of the interval and leave it. In Figure 7 (c), the population of differentiated cells in the middle of the interval becomes larger than before. There are also other differentiated cells which move to the borders of interval. This regime is not periodic anymore. Finally, for v_c sufficiently large differentiated cells appear only in the middle of interval.

3.3. **Quiescent state of cells.** In this model we suppose that cells can be either in quiescent state (type Q) or in cell cycle (type A). When a cell enters cell cycle, it grows and then divides into two identical to itself cells. We specify the model (1.1)-(1.3) in the following way. The equations which describe the evolution of the concentrations u and v in the extra-cellular matrix take the form:

$$\begin{cases} \dfrac{du}{dt} = d_1 \frac{\partial^2 u}{\partial x^2} + b_1^1 c_1 + b_1^2 c_2 - q_1 u, \\ \\ \dfrac{dv}{dt} = d_2 \frac{\partial^2 v}{\partial x^2} + b_2^1 c_1 + b_2^2 c_2 - q_2 v. \end{cases} \tag{3.20}$$

Here c_1 is the concentration of cells in cell cycle. We suppose that cells in quiescent state do not produce u and v. Therefore, $b_1^2 = b_2^2 = 0$. As before, we consider the no-flux boundary conditions.

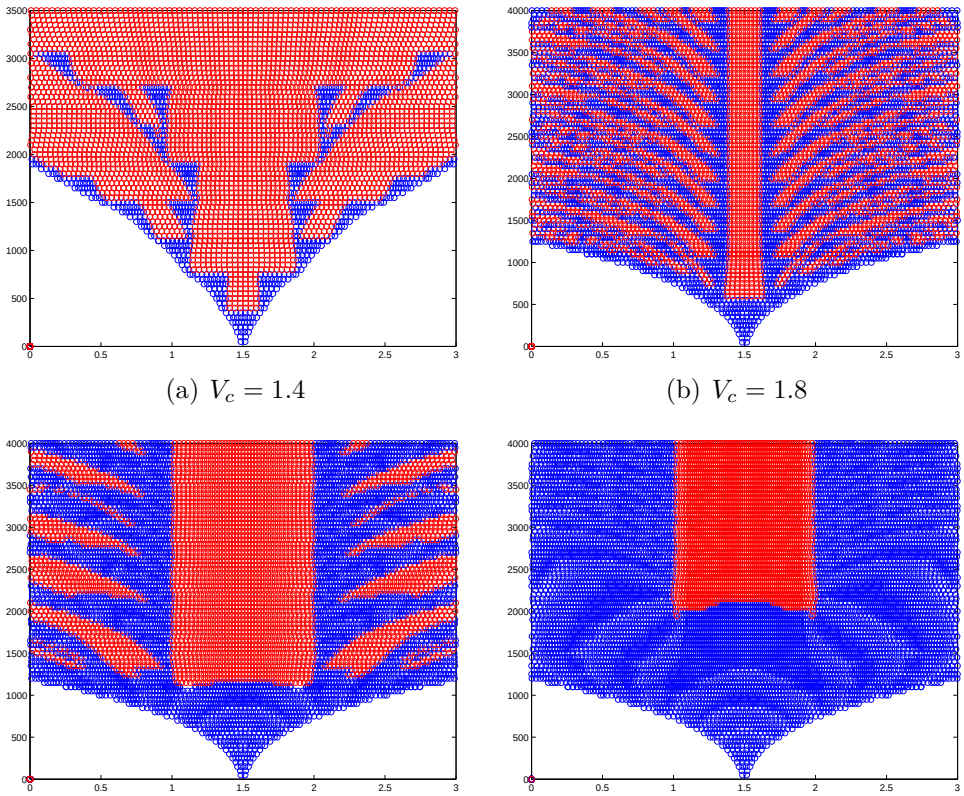

(a) $V_c = 1.4$ (b) $V_c = 1.8$

(c) $V_c = 3$ (d) $V_c = 8.2$

FIGURE 7. Evolution of cell population in the case of self-renewal and differentiation. Differentiated cells are shown in red; $k_1^{(1)} = -3 \cdot 10^{-3}$, $k_2^{(1)} = k_1^{(2)} = k_2^{(2)} = 0$, $K_3 = 10^{-3}$, $H_1 = 0.1$, $H_2 = 0.01$, $b_1 = 0.2$, $b_2 = 0.1$, $q_1 = 0.02$, $q_2 = 0.0001$, $D_2 = 1$.

Intra-cellular regulatory networks for the i-th cell in a cell cycle are described by system (3.21) of ordinary differential equations

$$\begin{cases} \dfrac{du_i}{dt} = k_1^{(u)} u(x,t) - k_2^{(u)} u_i(t) + H_u, \\ \\ \dfrac{dv_i}{dt} = k_1^{(v)} v(x,t) - k_2^{(v)} v_i(t) + H_v. \end{cases} \tag{3.21}$$

When the value of v_i overcomes v_c, the cell leaves cell cycle and becomes quiescent. It changes its type from A to Q. The intra-cellular concentrations for the i-th cell in a quiescent state is described by the equation:

$$\frac{dp_i}{dt} = k_1^{(p)} u(x,t) - k_2^{(p)} p_i(t) + H_p. \tag{3.22}$$

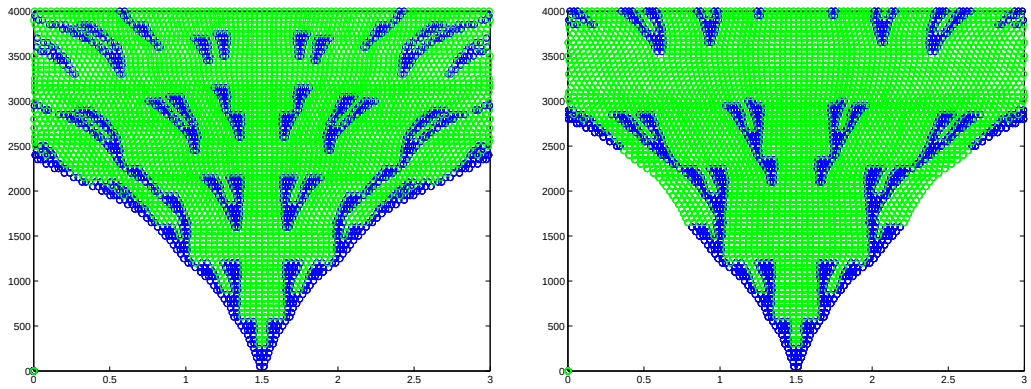

(a) $k_1^{(p)} = -7 \cdot 10^{-3}$ (b) $k_1^{(p)} = -1.8 \cdot 10^{-2}$

FIGURE 8. Evolution of cell population in the case where cells can self-renew (blue) or remain quiescent (green); $L = 3$, $k_1^{(u)} = -5 \cdot 10^{-3}$, $V_{crV} = 0.5$, $V_{crP} = 10$.

When p_i reaches the critical value p_c, the cell enters again cell cycle. Figure 8 presents two examples of this simulation. We observe that cells periodically enter and leave cell cycle.

4. 2D MODELLING.

4.1. **Cell differentiation and apoptosis.** We illustrate 2D simulation with one of the models considered in the previous section where cells can either self-renew or differentiate. Evolution of extracellular and intracellular concentrations is described by systems (3.18)-(3.19) where 1D diffusion is replaced by the 2D Laplace operator.

We start simulation with a single cell at the center of a square domain. Cells grow, divide and die resulting in the emergence of various patterns which can be radially symmetric, asymmetric or even chaotic depending on the value of parameters. Two examples are shown in Figure 9.

4.2. **Modelling of tumor growth.** In this section we consider the complete model (1.1)-(1.3) assuming that u is a scalar variable. It describes the concentration of nutrients which diffuse from the boundary of the domain and which are consumed by cells inside the domain. We consider the equation

$$\frac{\partial u}{\partial t} = D\ \Delta u - kcu, \tag{4.23}$$

where c is cell concentration and k is a positive parameter. The rate of nutrient consumption is proportional to the product of the concentrations. The form of the domain and of the boundary conditions will be specified below.

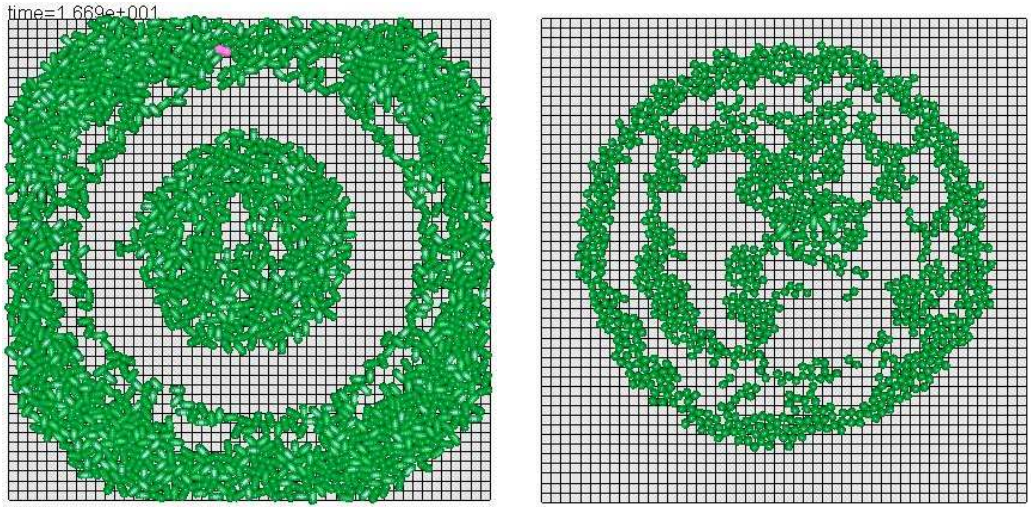

(a) $q_1 = 0.02$, $q_2 = 0.5$, $k_1^{(1)} = 0$, $k_1^{(2)} = 5$, $D_2 = 0.0001$, $V_{cr} = 1$

(b) $q_1 = -1$, $q_2 = -0.0001$, $k_1^{(1)} = -0.01$, $k_1^{(2)} = 0$, $D_2 = 1$, $V_{cr} = 1$

FIGURE 9. 2D simulations in the case of cell self-renewal and apoptosis; snapshots of cell populations. $H_1 = 0.1$, $H_2 = 0.01$, $b_1 = 0.2$, $b_1 = 0.1$, $k_2^{(2)} = k_2^{(1)} = 0$ $D_1 = 0.0001$

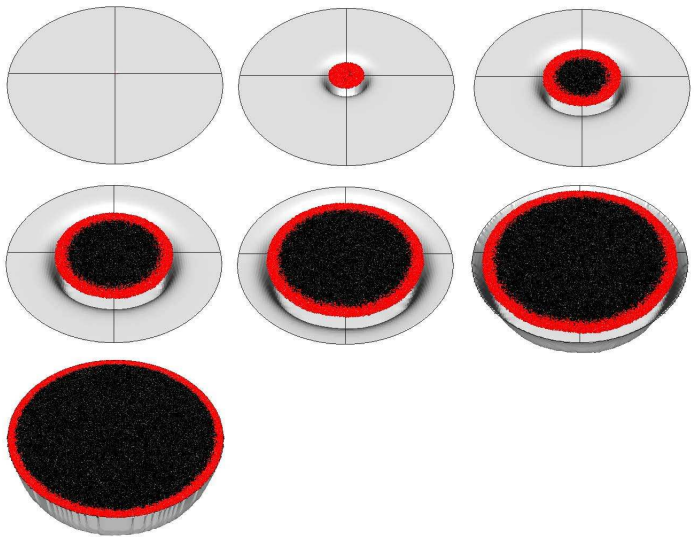

FIGURE 10. Consecutive moments of tumor growth. It starts with a single cell at the center of the circle. Living cells are shown in red, dead cells in black. 2D grey surface shows the level of nutrients.

Next, we consider the scalar intra-cellular variable u_i where the subscript i corresponds to the cell number. It is described by the equation

$$\frac{du_i}{dt} = k_1 u(x_i, t) - k_2 u_i. \tag{4.24}$$

The first term in the right-hand side of this equation shows that the intra-cellular concentration u_i grows proportionally to the value of the extra-cellular concentration $u(x,t)$ at the space point x_i where the cell is located. The second term describes consumption or destruction of u_i inside the cell. We suppose that the cell radius r_i grows proportionally to the increase of u_i:

$$\frac{dr_i}{dt} = \max\left(\frac{du_i}{dt}, 0\right). \tag{4.25}$$

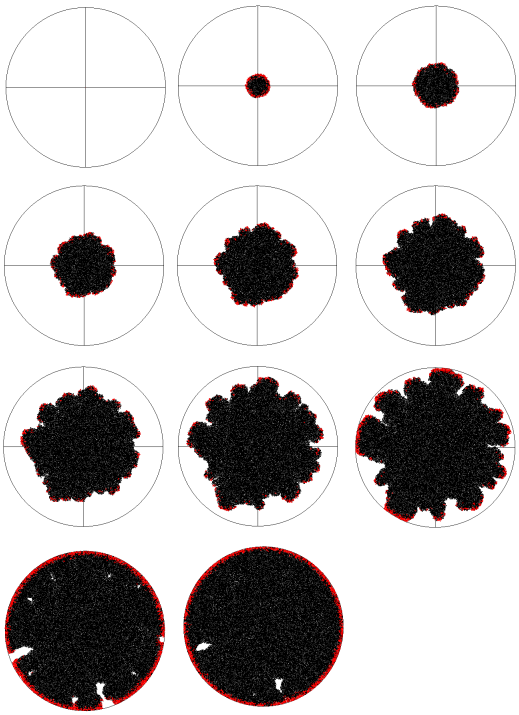

FIGURE 11. Consecutive moments of tumor growth. If the life time of cells is short, they become more sensitive to the lack of nutrient. The region filled by cells loses its radial symmetry.

The initial value of the radius for each new cell is r_0, the maximal radius r_m. When it is reached, the cell divides. If the cell does not divide before its maximal age, then it dies. The maximal cell age is a parameter of the problem.

Consider a circular domain Ω and complete equation (4.23) by the boundary condition $u = 1$ at the boundary $\partial\Omega$. We put a single cell in the center of the domain and begin numerical solution of system (4.23)-(4.25). The results of the simulations are shown in Figure 10 for several consecutive moments of time. The grey 2D surface shows the spatial distribution of the concentration $u(x,t)$. In the beginning it equals 1 everywhere in the domain. The constants k_1 and k_2, $k_1 > k_2$ are chosen in such a way that the intra-cellular concentration u_i

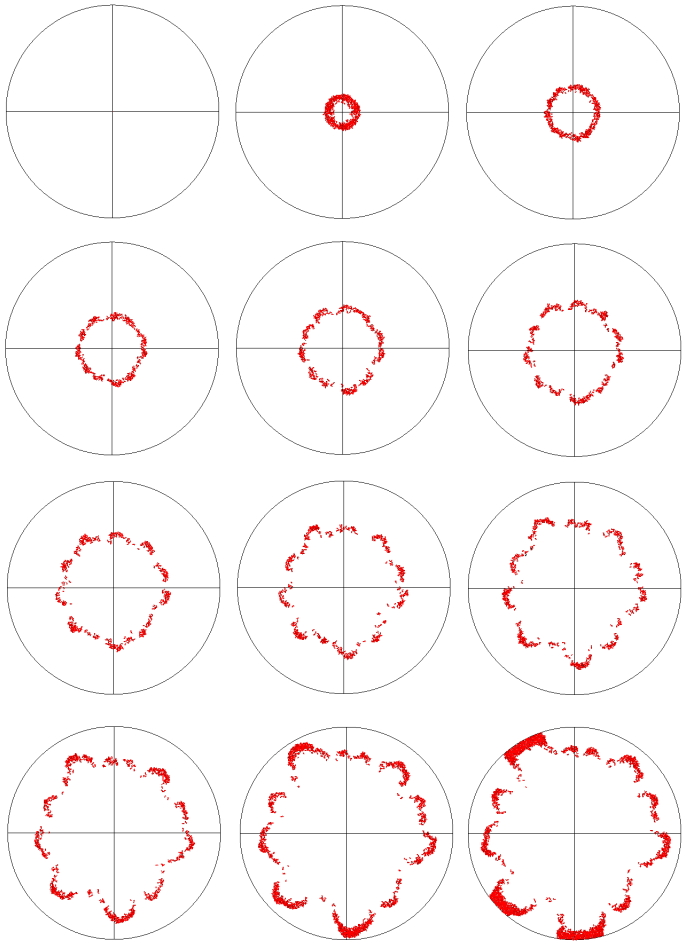

FIGURE 12. Living cells are shown in red. Dead cells are removed from the computational domain. The narrow region filled by cells is less stable and propagates with a smaller speed than in the presence of dead cells inside.

growth. Consequently, the radius of the cell also grows and after some time the cell divides. The new cells also consume nutrients, grow and divide. The part of the domain filled by cells forms a disk while the concentration $u(x,t)$ decreases in the center of the domain (second figure in the upper row). Hence, the right-hand side of equation (4.25) also decreases, the intra-cellular concentration stops growing or even decreases, and cells cannot divide before their maximal age τ. As a result, they die and form the black region in the center. Living cells shown in red form a narrow external layer. The region filled by cells grows in time and finally approaches to the boundary of the domain.

Dynamics of the cell population can be more complex if we decrease the maximal life time τ. Cells now have less time to accumulate enough nutrients for

division. In this case, even a small decrease in nutrient concentration can become crucial from the point of view of the choice between proliferation and apoptosis. In the beginning cells form, as before, a circular region with living cells outside and the core formed by dead cells. The layer of living cells is narrower than in the previous example. Rather rapidly the layer of living cells becomes disconnected (Figure 11, third in the upper row). After that the domain loses its radial symmetry which can be related to an instability with a certain wavenumber. Further growth of the region filled by cells makes the outgrowing parts more pronounced and this region less regular. Finally it reaches the boundary of the domain.

If dead cells are removed from the computational domain, then living cells can form a growing annulus or, when this regime becomes unstable, some narrow region filled by living cells and propagating from the center to the boundary of the domain (Figure 12).

References

[1] N. Bessonov, P. Kurbatova, V. Volpert. *Particle Dynamics Modelling of Cell Populations.*

[2] A. R. A. Anderson, K.A. Rejniaka, P. Gerleea, V. Quaranta. *Modelling of Cancer Growth, Evolution and Invasion: Bridging Scales and Models*, Math. Model. Nat. Phenom. **2(3)** (2007), 1–29

[3] A. R. A. Anderson, M. Chaplain, K.A. Rejniak, *Single Cell Based Models in Biology and Medicine* (Mathematics and Biosciences in Interaction), 2007

[4] H. G. Othmer, K. Painter, D. Umulis,C. Xue. *The Intersection of Theory and Application in Elucidating Pattern Formation in Developmental Biology*, Math. Model. Nat. Phenom. **4(4)** (2009), 3–82

[5] Dirk Drasdo, *Center-based single-cell models: An approach to multi-cellular organization based on a conceptual analogy to colloidal particles*, Mathematics and Biosciences in Interaction, 2007, 171–196

[6] Timothy J. Newman, *CModeling multicellular sructures using the subcellular element model*, Mathematics and Biosciences in Interaction, 2007, 221–239

[7] John C. Dallon, *Models with lattice-free center-based cells interacting with continuum environment variables*, 2007, 197–219

[8] Alexander R.A. Anderson, *A hybrid multiscale model of solid tumour growth and invasion: Evolution and the microenvironment*, Mathematics and Biosciences in Interaction, 2007, 3–28

[9] Andreas Deutsch, *Lattice-gas cellular automaton modeling of developing cell systems*, Mathematics and Biosciences in Interaction, 2007, 29–51

[10] Mark Alber, Nan Chen, Tilmann Glimm, Pavel Lushnikov, *Two-dimensional multiscale model of cell motion in a chemotactic field*, Mathematics and Biosciences in Interaction, 2007, 53–76

N. Bessonov
Institute of Mechanical Engineering Problems
199178 Saint Petersburg, Russia
Institut Camille Jordan
University Lyon 1
UMR 5208 CNRS
69622 Villeurbanne, France

P. Kurbatova,
Institut Camille Jordan
University Lyon 1
UMR 5208 CNRS
69622 Villeurbanne, France

V. Volpert
Institut Camille Jordan
University Lyon 1
UMR 5208 CNRS
69622 Villeurbanne, France